AIAA 81-1386R

Analysis of Combustion in Recirculating Flow for Rocket Exhausts in Supersonic Streams

A.C.H. Mace*
Ministry of Defence, Aylesbury, England
and
N.C. Markatos,† D.B. Spalding,‡ and D.G. Tatchell§
CHAM Ltd., London, England

A new computer program has been written to calculate the properties of the recirculating base flow region of a rocket exhaust plume. The nozzle stream and the freestream, either of which may be supersonic, mix turbulently to form an axisymmetric compressible free boundary layer. Solutions of the elliptic differential equations, which incorporate a two-equation model of turbulence closure, are obtained using an iterative finite-difference technique coupled to a point-by-point solution of the chemical kinetics. Predictions are presented for the velocity, pressure, temperature, and species concentration distributions in the base recirculation region of a rocket exhaust plume under supersonic flight conditions.

Nomenclature

a_n = area of finite-difference cell face n
A_n^ϕ = convection-diffusion coefficient in general finite-difference equation
A_P^ϕ = sum over transport coefficients at cells adjacent to position P
C_1, C_2, C_D = turbulence model constants
C_{p_i} = constant pressure specific heat of species i
C_{s_i}, C_{h_i} = integration constants for entropy and enthalpy definitions
f_i = time-averaged mass fractions of chemical species i
$f_{i,P}$ = modified mass fractions, used in chemical species equations
F_ϕ = function for Newton-Raphson solution
g_i = Gibbs free energy of species i
h = total enthalpy
h_i = enthalpy of species i
h_P^* = modified enthalpy, used in chemical species equations
k = turbulence kinetic energy
m_i = molecular weight of species i
m_P = source term of pressure correction equation at position P
p = pressure
r_{nozzle} = radius of nozzle in nozzle exit plane
r_{wall} = radius of missile in nozzle exit plane
r_{outer} = radial span of calculation domain
S_ϕ = source term of variable ϕ in finite-difference equation
S_1^ϕ, S_2^ϕ = coefficients of linearized source term
s_i = entropy of species i
T = time-averaged temperature
u = time-averaged axial velocity
v = time-averaged radial velocity
$\dot{w}_i$ = mass rate of production of species i
x_{outlet} = axial span of calculation domain
δ_n = distance between adjacent finite-difference cells
ϵ = turbulence energy dissipation rate
σ_ϕ = exchange coefficient for variable ϕ
ρ = time-averaged density
μ = effective viscosity coefficient
μ_l, μ_t = laminar and turbulent viscosity coefficients

Presented as Paper 81-1386 at the AIAA/SAE/ASME 17th Joint Propulsion Conference, Colorado Springs, Colo., July 27-29, 1981. Submitted August 5, 1981; revision received April 15, 1982.

*Senior Scientific Officer, Applied Combustion Section, Propellants, Explosives, and Rocket Motor Establishment.
†Technical Manager. Member AIAA.
‡Managing Director (Professor of Heat Transfer, University of London, England).
§Deputy Managing Director.

Introduction

TECHNIQUES for calculating the exhaust plume structure of a low-altitude tactical missile have been reported by Jensen and Wilson[1] and Jensen, Spalding, Tatchell, and Wilson.[2] In the former case, assumptions were made that the flowfield contained no radial pressure gradients and that the axial transport mechanism was dominated by convective rather than diffusive processes. The latter describes developments which overcame these assumptions; however the technique, when applied in its fully elliptic form, was very slow in obtaining a converged solution. This paper describes a new code which more efficiently computes flow and combustion in the recirculating region of the plume for a missile with a base radius significantly larger than the nozzle exit radius. The use of a Newton-Raphson technique to compute finite-rate chemistry point by point[3] reduces the time required to obtain a converged solution. Results of computations performed with this code are presented for representative supersonic flight conditions.

The Exhaust Structure

Calculations of rocket exhaust plume structures begin with predictions of chemical and hydrodynamical features within the combustion chamber and the nozzle. These provide nonequilibrium nozzle exit plane conditions which are used as input to the plume calculations. In the region of the exhaust where axial diffusion is important, it is necessary to solve elliptic differential equations using an iterative technique. Further downstream, where axial diffusion may be neglected, simpler parabolic differential equations may be used to describe the flow and are solved using a marching procedure.[1,2]

In a typical rocket exhaust plume, fuel-rich gases from the nozzle, at temperatures of 700-2500 K, mix turbulently with the cooler atmosphere. Recirculation will influence the flame properties, for instance, in determining whether combustion of the gases with entrained atmospheric oxidant will occur within the exhaust plume.

The flowfield around the missile base wall is shown in Fig. 1. The atmospheric flow, or freestream, and nozzle stream separate from the base at A and B, respectively, transferring momentum to the fluid in the trapped region by turbulent mixing. To preserve continuity, the flow dividing lines AC and BC meet at C, a stagnation point. The trapped gases circulate as a pair of vortices and an increase in pressure at C preserves this circulatory motion. The nature and extent of the flow pattern in the region ABC will depend upon the magnitude of the nozzle and freestream velocities. The recirculation provides a mechanism of accelerating mixing of fuel and oxidant and the base region may thereby act as a flame holder. The pressure immediately downstream of the base wall is lower than the freestream pressure and as such will contribute to the overall missile drag.

Mathematical Model

Hydrodynamics

Features of the exhaust plume to be predicted include time mean values of temperature, pressure, chemical species concentrations, and axial and radial velocities for missile flight velocities up to Mach 3. They are calculated from the conditions in the plane of the nozzle exit, along with a suitable reaction mechanism. The flow is considered as axisymmetric and free of condensed species.

The partial differential equations describing the fluid dynamics of the plume are written in the following two-dimensional form with axial and radial coordinates x and r, respectively,[2]

$$\frac{\partial}{\partial x}(\rho u\phi)+\frac{1}{r}\frac{\partial}{\partial r}(r\rho v\phi)-\frac{\partial}{\partial x}\left(\frac{\mu}{\sigma_\phi}\frac{\partial\phi}{\partial x}\right)-\frac{1}{r}\frac{\partial}{\partial r}\left(\frac{r\mu}{\sigma_\phi}\frac{\partial\phi}{\partial r}\right)=S_\phi \tag{1}$$

This represents the transport equation for a general variable ϕ. The variables u and v are axial and radial velocity components, ρ is the density, μ the effective viscosity coefficient, and σ_ϕ the ratio of the rate of exchange of ϕ to the rate of exchange of momentum. The final term, S_ϕ, is the source term and is expressed in Table 1 for the hydrodynamic variables required.

The equations for momenta and enthalpy are closed using the viscosity-stress relation of Reynolds. The effective viscosity coefficient is defined and calculated from the two-equation model of turbulence, using the turbulence kinetic energy k and its dissipation rate ϵ,[4]

$$\mu=(C_D\rho k^2)/\epsilon+\mu_l \tag{2}$$

where C_D is an empirical constant, μ_l is the laminar viscosity coefficient, and k and ϵ are evaluated using Eq. (1) and source terms in Table 1. The values for C_1 and C_2 in jet boundary layers are considered by Pope[5]; however, in the analysis reported here, fixed values of C_1 and C_2 are used at all positions in the calculation domain.

Further relationships are required for: 1) the density of the gas, from the ideal gas equation; 2) the pressure, by applying the continuity condition to all local fluid volumes; and 3) the temperature, from the enthalpy and species concentrations.

Chemistry

The enthalpy h_i, entropy s_i, and Gibbs free energy g_i for a chemical species i are written

$$h_i=\int C_{p_i}\mathrm{d}T+C_{h_i} \tag{3}$$

$$s_i=\int C_{p_i}\frac{\mathrm{d}T}{T}+C_{s_i} \tag{4}$$

$$g_i=h_i-Ts_i \tag{5}$$

where C_{pi} is the constant pressure specific heat of the ith species, T the time-averaged temperature, and C_{h_i} and C_{s_i} integration constants defined from the enthalpies of formation. The total enthalpy is then defined as

$$h=\sum_i f_i h_i(T)+\frac{u^2+v^2}{2}+k \tag{6}$$

where f_i is the mass fraction of species i. The temperature is recovered from Eqs. (3-6) by iteration, until the right side of Eq. (6) agrees with the solution of the transport equation (1) for enthalpy.

The species concentrations are computed from the conservation transport equation (1) with $\phi=f_i$, the time-averaged species mass fraction, and $S_\phi=\dot{w}_i$, the mass rate of production of species i from other chemical species. All the

Table 1 Source terms of dependent variables

Variable ϕ	Source term S_ϕ
Axial velocity u	$-\frac{\partial p}{\partial x}+\frac{\partial}{\partial x}\left(\mu\frac{\partial u}{\partial x}\right)+\frac{1}{r}\frac{\partial}{\partial r}\left(r\mu\frac{\partial v}{\partial x}\right)$
Radial velocity v	$-\frac{\partial p}{\partial r}-2\frac{\mu v}{r^2}+\frac{\partial}{\partial x}\left(\mu\frac{\partial u}{\partial r}\right)+\frac{\partial}{\partial r}\left(r\mu\frac{\partial v}{\partial r}\right)$
Total enthalpy h	$\frac{1}{r}\frac{\partial}{\partial r}\left[r\mu\left(1-\frac{1}{\sigma_h}\right)\frac{\partial}{\partial r}\left(\frac{u^2}{2}\right)\right]+\frac{1}{r}\frac{\partial}{\partial r}\left[r\mu\left(\frac{1}{\sigma_k}-\frac{1}{\sigma_h}\right)\frac{\partial k}{\partial r}\right]$
Turbulence kinetic energy k	$\mu_t\left\{2\left[\left(\frac{\partial u}{\partial x}\right)^2+\left(\frac{\partial v}{\partial r}\right)^2\right]+\left(\frac{\partial u}{\partial r}+\frac{\partial v}{\partial x}\right)^2+\frac{2v^2}{r^2}\right\}-\rho\epsilon$
Dissipation of turbulence kinetic energy ϵ	$\frac{\epsilon C_1\mu_t}{k}\left\{2\left[\left(\frac{\partial u}{\partial x}\right)^2+\left(\frac{\partial v}{\partial r}\right)^2\right]+\left(\frac{\partial u}{\partial r}+\frac{\partial v}{\partial x}\right)^2+\frac{2v^2}{r^2}\right\}-\frac{C_2\rho\epsilon^2}{k}$

Note: Where p is the pressure, C_1 and C_2 empirical coefficients, and μ_t the turbulent eddy viscosity coefficient, the first term of Eq. (2).

effects of finite-rate chemical reactions are contained within the source terms $\dot{w}_i$, as described elsewhere.[1,2]

Method of Solution

Finite-Difference Equations

Equation (1) may be written in finite-difference form by multiplying by r and integrating over an elemental cell volume surrounding a defined point P,[6]

$$\sum_n (A_n^\phi - S_2^\phi)\phi_P = \sum_n A_n^\phi \phi_n + S_1^\phi \tag{7}$$

where the summation n is over the cells adjacent to P. The coefficients A_n^ϕ, which account for convective and diffusive mass fluxes across the elemental cell, are formulated using upwind differencing. For example, the coefficient for the high-x neighbor is

$$A_n^\phi = \left(\frac{\mu}{\sigma_\phi}\right)_n \frac{a_n}{\delta_n}, \text{ when } u_n < 0$$

and

$$A_n^\phi = \rho_P u_n a_n + \left(\frac{\mu}{\sigma_\phi}\right)_n \frac{a_n}{\delta_n}, \text{ when } u_n \geq 0$$

where δ_n is the distance between nodes P and n, a_n the area of the cell face, $(\mu/\sigma_\phi)_n$ the arithmetic mean of the values at P and n, and ρ_P the upwind value of density (in this case that at grid node P). The source term is written in the linear form $S_\phi = S_1^\phi + \phi S_2^\phi$.

The pressure field is obtained from a pressure correction equation,

$$\sum_n A_n^\phi p_P' = \sum_n A_n^\phi p_n' + m_P \tag{8}$$

where m_P is the local mass continuity error for cell P, and p_P' the pressure correction to be applied at P. Equation (8) is derived from Eq. (1) for mass continuity and is used to compute the pressure change required to produce velocities and densities which preserve continuity.[6]

Newton-Raphson Solution for Chemical Species Concentrations

At many positions in the rocket exhaust plume, chemical reaction rather than turbulent mixing dominates local variations of species concentrations and $f_{i,P}$, the mass fraction of species i at position P, will depend more strongly on other species concentrations and temperatures at P than on $f_{i,n}$ in adjacent cells.

In the earlier programs[1,2] the species mass fractions were evaluated from the transport equation with the reaction rate source terms treated explicitly. Faster convergence is obtained by solving species concentrations simultaneously at each cell by the point-by-point procedure developed by Pratt and Wormeck.[3] This procedure may be summarized as follows.

Equation (7) is written, for species mass fractions at P,

$$\sum A_n^{f_i}\left(f_{i,P} - \frac{\sum_n A_n^{f_i} f_{i,n}}{\sum_n A_n^{f_i}}\right) = S_{f_{i,P}} \tag{9}$$

and similarly for enthalpy,

$$\sum A_n^h\left(h_P - \frac{\sum_n A_n^h h_n}{\sum_n A_n^h}\right) = S_{h,P} \tag{10}$$

These may be reduced to the simpler form,

$$A_P^{f_i}(f_{i,P} - f_{i,P}^*) = S_{f_{i,P}} \tag{11}$$

$$A_P^h(h_P - h_P^*) = S_{h,P} \tag{12}$$

where

$$A_P^\phi = \sum_n A_n^\phi, \; f_{i,P}^* = \left(\sum_n A_n^{f_i} f_{i,n}\right) \Big/ A_P^{f_i},$$

and

$$h_P^* = \left(\sum_n A_n^h h_n\right) \Big/ A_P^h$$

At each position, A_P^ϕ is fixed and the species mass fractions depend only on other species, interacting through the chemical reactions contained within the source term.

A functional expression

$$F_\phi = A_P^\phi(\phi_P - \phi_P^*) - S_\phi \tag{13}$$

is defined along with suitable starting values, and a Newton-Raphson scheme is employed which solves iteratively for all ϕ_i until the matrix elements of F_ϕ are sufficiently small.[3] The final solution is completely consistent with the fully converged simultaneous solutions of the transport equations (1). The use of this Newton-Raphson procedure to compute point-by-point converged chemistry solutions typically reduces the computation time to less than 20% of that required to converge the species conservation equations alone.

Boundary Conditions

The boundary conditions relate to the solution domain of Fig. 2. This extends axially from an inlet plane coplanar with the rocket nozzle exit, to an outlet plane downstream from the recirculation region. The radial extent is from the symmetry axis to an outer location beyond the missile base radius and sufficient to enclose the expanding plume.

With $\phi(x,r)$ referring to any variable at position (x,r), and $\phi_\infty = \phi(0, r > r_{\text{wall}})$, the boundary conditions are as follows:

1) Symmetry axis, $r = 0$; $v = 0$, $\partial\phi/\partial r = 0$.

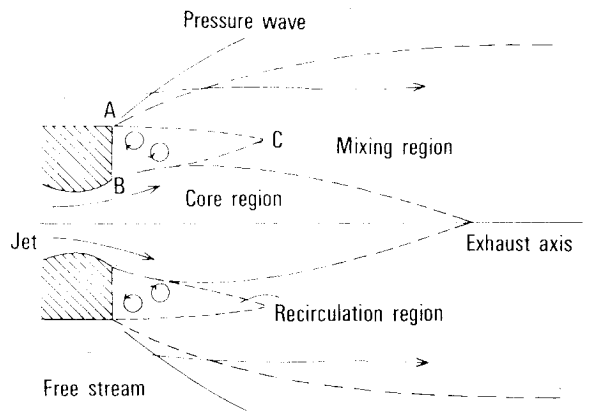

Fig. 1 Flowfield around the missile base wall.

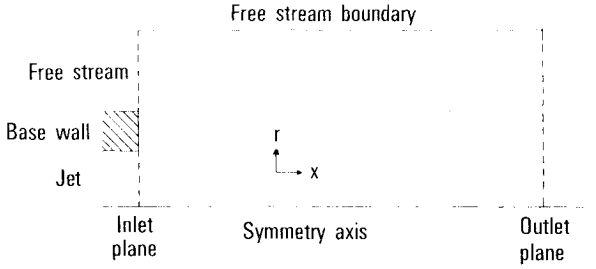

Fig. 2 The solution domain.

Table 2 Conditions at the inlet of the calculation domain

Variable ϕ	Nozzle stream values	Freestream values
Chemical species concentrations, molecule·cm^{-3}		
N_2	1.2×10^{18}	2.0×10^{19}
O_2	5.5×10^{12}	5.3×10^{18}
CO	3.3×10^{18}	–
H_2	8.2×10^{17}	–
OH	5.1×10^{13}	–
H	2.5×10^{15}	–
O	1.4×10^{11}	–
H_2O	2.3×10^{18}	–
CO_2	1.5×10^{18}	–
Axial velocity, ms^{-1}	2000.0	1000.0
Radial velocity, ms^{-1}	0.0	0.0
Pressure, kN·m^{-2}	150.0	101.0
Temperature, K	1200.0	288.0
Mach number	2.72	2.88
Density, kg·m^{-3}	0.39	1.16
Radius of nozzle exit, m	0.1	–
Radius of missile, m	0.4	–

Note: All variables are set uniformly across the nozzle exit plane and freestream inlet boundary.

Table 3 Turbulence model data

Turbulence constants		Exchange coefficients	
C_1	1.44	σ_h	0.9
C_2	1.92	σ_k	1.0
C_D	0.09	σ_ϵ	1.3
		σ_{f_i}	0.9

Table 4 The chemical reaction mechanism

Reaction[a]	Forward rate coefficient[b]	Uncertainty factor
$O+O+M\rightarrow O_2+M$	$1\times10^{-29}T^{-1}$	30
$O+H+M\rightarrow OH+M$	$1\times10^{-29}T^{-1}$	30
$H+H+M\rightarrow H_2+M$	$5\times10^{-29}T^{-1}$	30
$H+OH+M\rightarrow H_2O+M$	$2\times10^{-28}T^{-1}$	10
$CO+O+M\rightarrow CO_2+M$	$1\times10^{-29}T^{-1}\exp-1250/T$	30
$OH+H_2\rightarrow H_2O+H$	$3.6\times10^{-11}\exp-2600/T$	3
$O+H_2\rightarrow OH+H$	$2.9\times10^{-11}\exp-4730/T$	3
$H+O_2\rightarrow OH+O$	$3.7\times10^{-10}\exp-8400/T$	3
$CO+OH\rightarrow CO_2+H$	$9\times10^{-13}\exp-540/T$	5
$OH+OH\rightarrow H_2O+H$	$1\times10^{-11}\exp-390/T$	5

[a] M is an exhaust flame molecule.

[b] Rate coefficients are in ml·molecule·s units.

2) Outer boundary, $r=r_{\text{outer}}$; $\phi=\phi_\infty$, except v; subsonic freestream, $v=0$; supersonic freestream, $v=v_\infty+[(p-p_\infty)/\rho_\infty u]\ (M^2-1)^{1/2}$, where M is the freestream Mach number at the inlet plane.[7]

3) The outlet boundary, $x=x_{\text{outlet}}$; $\partial\phi/\partial x=0$, except for subsonic freestream pressure $p=p_\infty$.

4) The inlet boundary, $x=0$; $r\geq r_{\text{wall}}$, $\phi=\phi_\infty$; $r\leq r_{\text{nozzle}}$, $\phi=\phi_{\text{jet}}$; $r_{\text{wall}}>r>r_{\text{nozzle}}$, $u=0$; v, k, and ϵ are defined using logarithmic wall functions.[6]

The jet and freestream inlet values of turbulence kinetic energy and its dissipation rate are defined, for calculations reported here, as

$$k_{\text{inlet}}=0.005\,u^2_{\text{inlet}} \tag{14}$$

and

$$\epsilon_{\text{inlet}}=C_D k^{3/2}_{\text{inlet}}/0.1\,r_{\text{nozzle}} \tag{15}$$

This may not be satisfactory for the freestream and further comparisons with experimental results will be required to improve this selection.

Solution Procedure

The following sequence is used to obtain solutions for all variables associated with hydrodynamics and chemistry:

1) The conservation equations are solved for u, v, k, ϵ, h, and f_i for all species, using the Jacobi procedure[8] for u and v and the tridiagonal matrix algorithm (TDMA)[9] for the remaining variables. These equations are solved simultaneously in the r direction at a constant x line for constant temperature, pressure, and density.

2) The values of f_i and temperature are modified simultaneously using Eqs. (11-13) and the Newton-Raphson procedure to obtain a converged point-by-point solution for the chemistry at each radial position. The f_i's computed from TDMA are used as initial values.

3) The temperature, density, and viscosity are evaluated along the radial line and the source terms for the pressure correction computed.

4) Steps 1-3 are repeated at successive axial positions from the inlet plane to the outlet plane.

5) The pressure field is computed for the whole field to suppress mass continuity errors that have accumulated during the previous steps and u and v are then updated.

6) Steps 1-5 are repeated until a converged solution is obtained.

Initial Conditions

The calculation is initiated from guessed values of all variables at every position in the calculation domain: $r<r_{\text{nozzle}}$, $\phi(x,r)=\phi\ (0,0)$; $r\geq r_{\text{nozzle}}$, $\phi(x,r)=\phi_\infty$. The converged solutions are independent of initial values; however, the choice influences the time taken to obtain convergence.

Computational Details

The described prediction techniques have been used to compute the structure of rocket exhaust plumes for supersonic and subsonic flight missiles with base recirculation. The nozzle exit plane and freestream conditions of the principal calculation presented here are listed in Table 2; these are typical of a tactical missile traveling at Mach 2.9 at sea level. The ratio of the base diameter to the nozzle exit diameter is 4,

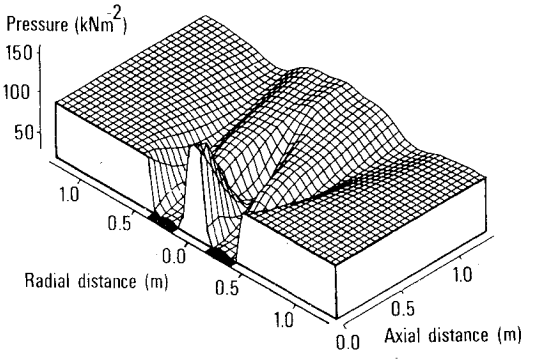

Fig. 3 Isometric projection of the pressure field for conditions of Table 2 (the base region is indicated with shading).

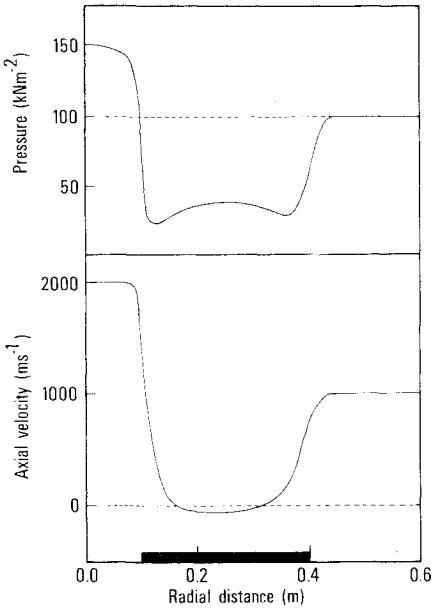

Fig. 4 Radial profiles of pressure and axial velocity at an axial distance 0.02 m downstream of the nozzle exit plane, for conditions in Table 2 (the shaded area represents the base region).

and a recirculation region exists close to the missile base. No allowance is made for the boundary layer attached to the missile body, or for any other perturbations to the freestream flow which would influence the inlet conditions for the calculation. All variables across the nozzle and freestream inlet are set uniformly to those of the jet and ambient conditions, respectively.

The turbulence model constants used in the computations are listed in Table 3[4,6]; the value C_l, namely 1.44, is that used in other exhaust calculations.[2]

The nozzle exit flow contains significant mass fractions of fuel species H_2 and CO. The reactions used in the plume are presented in Table 4,[10] along with rate coefficients and uncertainty factors, and represent the important finite-rate chemical reactions for H_2 and CO combustion with O_2. The differences between these data and a more recent compilation[11] are not significant in these computations. The uncertainty factors provide rough upper and lower bounds to the rate coefficients. Thermochemical data for the gas-phase species were taken from the JANAF tables.[12]

The computational grid spanned 1.7 m radially with 17 grid positions, and 2.5 m axially with 21 grid positions. The distribution of the grid points was uniform, except within a region approximately 0.5 m square, extending symmetrically from the base wall, in which the grid spacing was half that employed elsewhere. The solution domain was chosen to

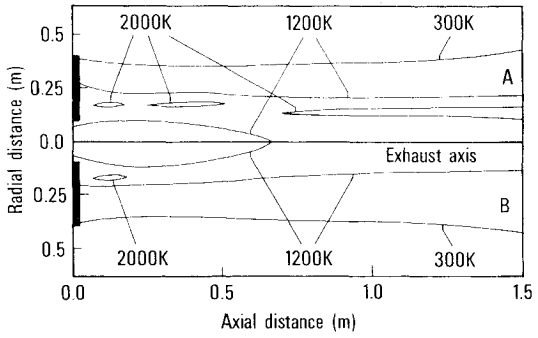

Fig. 5 Temperature field plotted as isothermal contours: A) calculation with full finite rate chemistry; B) calculation with inert treatment of chemical species (the shaded areas represent the base wall).

enclose the plume expansion, enabling the calculation to be continued beyond the outlet plane with a marching parabolic technique. The predictions of primary flow characteristics, such as the vortex structure, were insensitive to the grid specification; however, the grid used in these calculations was too coarse to enable detailed features of the shock structure to be predicted accurately.

In the calculations considered here, 200 iteration cycles of the form described in the previous section were sufficient to converge results to 0.01% in pressure and species concentrations. The computer time for such a calculation was equivalent to 15 min on a CDC-6600 computer. A similar calculation, solving just hydrodynamic equations for chemically inert flow, was 30 s on the same computer.

Results

A calculation for the conditions described predicts a region of subsonic flow which extends 1.8 m downstream from the nozzle exit plane and contains a recirculation region which extends 0.1 m from the base wall. The pressure field for this exhaust is plotted isometrically in Fig. 3. This map is symmetric about the plume axis and the base wall is identified by the shaded area. The pressures in the nozzle exit, the freestream, and just downstream of the base wall are 150, 101, and 36 kN·m^{-2}, respectively. As the nozzle flow expands into the base region the pressure on the plume axis decreases to a minimum, 44 kN·m^{-2}, at a distance 0.4 m downstream of the exit plane. The expanding flow is then reflected back from the recirculating region to the plume axis, giving rise to a peak axial pressure of 118 kN.m^{-2} roughly 1.1 m downstream of the nozzle exit plane.

In Fig. 4 the radial profiles of pressure and velocity are presented for an axial distance 0.02 m downstream of the nozzle exit plane. Across the center of the base wall the axial velocity is negative, corresponding to two counter-rotating vortices with centers of rotation 0.18 and 0.32 m from the plume axis and 0.05 m downstream from the nozzle exit plane. The pressure profile shows a small decrease in pressure toward the edges of the wall, the gradient of which drives the recirculating flow. The difference between the base wall and ambient pressures will contribute to the missile drag.

The isothermal contours in Fig. 5 describe the distribution of temperatures in the exhaust. The base wall region is again indicated by shading and the gas streams are moving from left to right. The upper half (A) represents the results for the conditions of Table 2, with a full treatment of the chemistry, and the lower half (B) shows the results for a calculation with inert gas streams of N_2 and identical hydrodynamic conditions. In the exhaust with chemically reacting flow (A), the temperature is predicted to increase significantly in a region about 0.7 m downstream of the nozzle exit and 0.15 m radially from the plume axis; this corresponds to the initiation of secondary combustion in the plume. The ratio of the width of

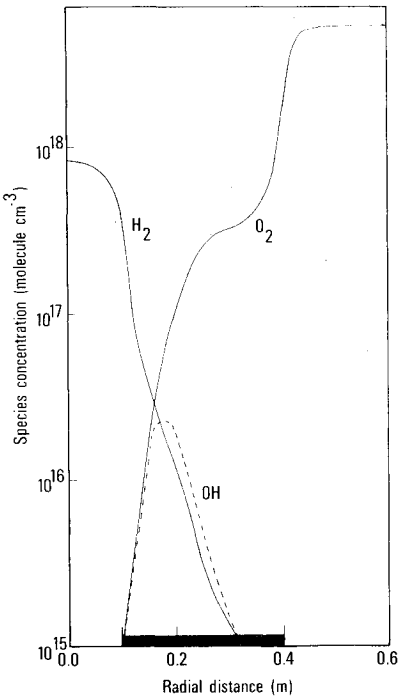

Fig. 6 Radial profiles of H_2, O_2, and OH at an axial distance 0.05 m downstream of the base wall (the shaded area represents the base region).

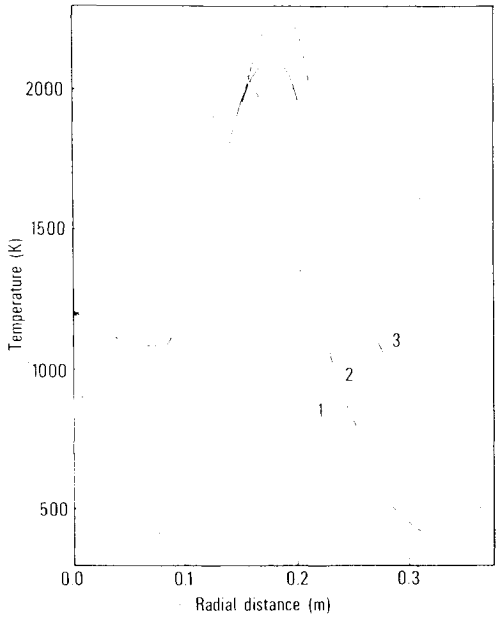

Fig. 7 Radial profiles of temperature at an axial station 0.1 m downstream of the nozzle exit plane [conditions are as in Table 2, except for the freestream axial velocities which are: 1) 300 ms^{-1}, 2) 500 ms^{-1}, 3) 1000 ms^{-1}].

the combustion region to the width of the exhaust plume increases with greater axial distance, and beyond 2.5 m (not shown on the figure) the combustion zone extends across the whole flow. This is absent in the predictions for inert flow (B).

The temperatures near the base wall are higher than those in the nozzle streams for both reacting and nonreacting predictions. This is a hydrodynamical feature of the flow and may be considered in more detail. The kinetic energy per unit mass in the nozzle stream $[(u^2+v^2)/2]$ is 2×10^6 m^2.s^{-2}, while in the region of vorticity it is 2×10^4 m$^2\cdot$s^{-2}. If the nozzle stream is inert the heat content per unit mass (C_PT)

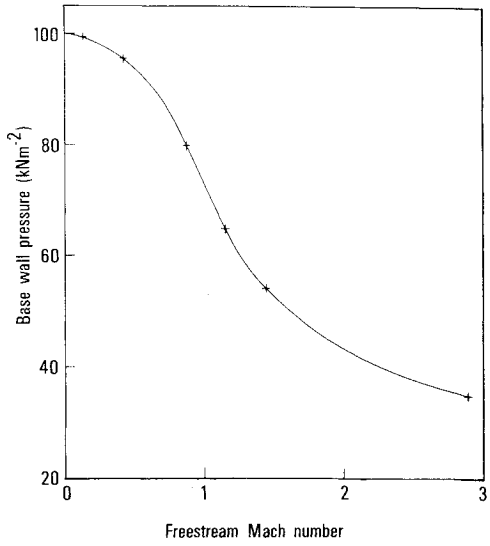

Fig. 8 The pressure, at a midradial point on the base wall, as a function of freestream Mach number.

is roughly $1500\times1200=1.8\times10^6$ m$^2\cdot$s^{-2}. The total enthalpy of the nozzle stream is then $2\times10^6+1.8\times10^6=3.8\times10^6$ m$^2\cdot$s^{-2}. At a position in the base region $r=0.2$ m, $x=0.02$ m, the enthalpy is computed to be 2.8×10^6 m$^2\cdot$s^{-2}, which implies a temperature of $(2.8\times10^6-2\times10^4)/1500=1870$ K. Similarly for chemically reacting flow, while the flow kinetic energy forms a significant fraction of the total energy in the nozzle and freestream, it is a much smaller fraction in the vortex region, leading again to high temperatures.

In Fig. 6 radial profiles of H_2, O_2, and OH are plotted for an axial distance 0.05 m downstream of the nozzle exit plane. The species represent typical fuel, oxidant, and free radial. The presence of the base wall generating recirculation enhances mixing of fuel and oxidizer. This enhanced mixing couples to the higher temperatures in the base region and provides a mechanism for rapidly producing excess free radical species which are important for the ignition of combustion. The onset of secondary combustion, see Fig. 5 (upper half), occurs at a radical distance almost coincident with the peak in radial distribution of [OH]. The difference between the concentration of O_2 at $r=0.3$ and 0.5 m is largely due to the steep gradients of pressure temperature and density in this region.

Further calculations were performed using the conditions of Table 2 and freestream axial velocities of 500, 400, and 300 ms^{-1} corresponding to Mach numbers 1.4, 1.1, and 0.9, respectively. Secondary combustion was predicted in all cases. However the position of the ignition and the values of the peak temperature varied by a small amount, the latter for instance by about 300 K. In Fig. 7 the radial temperature profiles at a position 0.1 m downstream of the base wall are plotted for three freestream velocities 300, 500, and 1000 ms^{-1}.

Finally in Fig. 8, the pressure at a midradial point on the base wall is plotted as a function of freestream Mach number. The results have been extended to zero using calculations with subsonic freestream velocities of 50 and 150 ms^{-1}. While no direct experimental verification of these predictions is available, the dependence of base pressure on the freestream Mach number is in quantitative agreement with wind-tunnel measurements made on projectiles with base diameters comparable to the width of the missile base wall.[13,14]

Conclusions

A method of calculating the structure of recirculation regions close to the base walls in turbulent, chemically

reacting rocket exhausts has been described. Its application to supersonic missiles has been illustrated. The computer code based on the method developed is a significant improvement on previous methods: run times are relatively short and storage requirements acceptable. Presently, however, the code is limited to axisymmetric gas-phase flow.

Acknowledgment

The authors are grateful to Dr. D.E. Jensen for many useful comments on the manuscript.

References

[1] Jensen, D.E. and Wilson, A.S., "Prediction of Rocket Exhaust Flame Properties," *Combustion and Flame,* Vol. 25, 1975, pp. 43-55.

[2] Jensen, D.E., Spalding, D.B., Tatchell, D.G., and Wilson, A.S., "Computation of Structures of Flames with Recirculating Flow and Radial Pressure Gradients," *Combustion and Flame,* Vol. 34, 1979, pp. 309-326.

[3] Pratt, D.T. and Wormeck, J., "CREK: A Computer Program for Calculation of Chemical Reaction Equilibrium and Kinetics in Laminar and Turbulent Flows," Dept. of Mechanical Engineering, Washington State University, Pullman, Rept. WSU-M-TEL-76-1, 1976.

[4] Launder, B.E. and Spalding, D.B., *Mathematical Models of Turbulence,* 1st Ed., Academic Press, London and New York, 1972.

[5] Pope, S.B., "An Explanation of the Turbulent Round-Jet/Plane-Jet Anomaly," *AIAA Journal,* Vol. 16, 1978, pp. 279-281.

[6] Patankar, S.V. and Spalding, D.B., "A Calculation Procedure for Heat, Mass and Momentum Transfer in Parabolic Flows," *International Journal of Heat and Mass Transfer,* Vol. 15, 1972, pp. 1787-1806.

[7] Markatos, N.C., Spalding, D.B., Tatchell, D.G., "Combustion of Hydrogen Injected into a Supersonic Airstream," NASA CR-2802, 1977.

[8] Smith, D.G., *Numerical Solutions of Partial Differential Equations,* 2nd Ed., Oxford University Press, Oxford, England, 1975.

[9] Hildebrand, F.B., *Introduction to Numerical Analysis,* 2nd Ed., McGraw-Hill Book Co., New York, 1974.

[10] Jensen, D.E. and Jones, G.A., "Gas Phase Reaction Rate Coefficients for Rocketry Applications," Ministry of Defence, Great Britain, RPE Tech. Rept. 71/9, 1971.

[11] Jensen, D.E. and Jones, G.A., "Reaction Rate Coefficients for Flame Calculations," *Combustion and Flame,* Vol. 32, 1978, pp. 1-34.

[12] JANAF Thermochemical Tables, 2nd Ed., National Bureau of Standards, Washington, D.C., NBS NSRDS No. 37, 1971.

[13] Cassanto, J.M., "Ratio on Base Pressure," *AIAA Journal,* Vol. 3, 1965, pp. 2351-2352.

[14] McDonald, H., "The Turbulent Supersonic Base Pressure Problem: A Comparison Between a Theory and Some Experimental Evidence," *Aeronautical Quarterly,* Vol. 17, 1966, pp. 105-126.